HASIL CEK6_60010383

by 60010383 Anton Yudhana

Submission date: 14-Jun-2022 11:16AM (UTC+0700)
Submission ID: 1856483545
File name: CEK 6_60010383.pdf (2.42M)
Word count: 8934
Character count: 44944

Sensing and Bio-Sensing Research 33 (2021) 100435

Contents lists available at ScienceDirect

Sensing and Bio-Sensing Research

journal homepage: www.elsevier.com/locate/sbsr

GIS-based and *Naïve Bayes* for nitrogen soil mapping in Lendah, Indonesia

Anton Yudhana [a,*], Dedy Sulistyo [a], Ilham Mufandi [b]

[a] Department of Electrical Engineering, Universitas Ahmad Dahlan Yogyakarta Kampus IV, Jl. Ringroad Selatan, Kragilan, Tamanan, Banguntapan, Bantul, Special Region of Yogyakarta 55191, Indonesia
[b] Department of Chemical Engineering, Indian Institute of Technology Delhi, New Delhi 110016, India

ARTICLE INFO

Keywords:
Geographical Information Systems (GIS)
Naïve Bayes
Soil Nitrogen
Rice

ABSTRACT

Rice or *Oryza sativa* L. is the staple food of Indonesian society. Currently, the demand for rice in Indonesia is increasing, while the level of rice production is decreasing. Therefore, alternative technologies are needed to assist the community in increasing rice production. One of the important factors in the growth of rice is the quality of the soil that contains high levels of nitrogen for photosynthesis, protein formation, acid formation, and accelerating plant growth. This research was applied for soil nitrogen mapping with a smart prototype using the TCS3200 sensor combined with Naive Bayes algorithm and GIS (Geographical information systems). This system is carried through the Wemos D1 Mini microcontroller of TCS3200 sensor for reading data and sending the data to the web ceerduad.com. Geographical information systems (GIS) was developed to mapping area and to obtain training data for the Naïve Bayes Algorithm which the researcher took 20 soil samples in Lendah sub-district. From the experiment results, a prototype of soil nitrogen content using the TCS3200 sensor can measure soil nitrogen levels with an accuracy of 87.5% and sending the sensor data to the web server. Implementation of GIS in this research was successfully mapping low, medium, and high levels of nitrogen.

1. Introduction

Rice or *Oryza sativa* L. is growing abundant in Indonesia as the society's staple food. However, farmers need to maintain rice plants to get the rice's good quality [1]. Currently, the demand for rice in Indonesia is increasing, while the level of rice production is decreasing. Therefore, alternative technologies are needed to assist the community in increasing rice production. One of the important factors in the growth of rice is the quality of the soil that contains high levels of nitrogen for photosynthesis, protein formation, acid formation, and accelerating plant growth. According to the publication of the Central Statistics Agency (BPS), national rice production in 2017 reached 47.30 million tons [2]. Generally, rice production depends on the season to produce rice's good quality in a tropical country like Indonesia [3]. There is the different of nitrogen soil level between rainy season and dry season [4]. Rice plants grow faster and huge good production In rainy season. [5]. Hence, measurement of soil level is important to improve the production, management, and planning agriculture activity [6].

The influence of the changing seasons during the rice planting can reduce rice production [7,8]. Therefore, farmers should develop agriculture method and technology to complete the rice consumption by increasing rice cultivation [9]. As a tropical country, Indonesia has unpredictable weather that can affect agricultural production, especially rice production, caused by annual rainfall [10], El Nino [11] and the temperature rise as the climate change [12]. In other hand, soil fertility is also influential on the rice production [13] and needed more attention to identify the plant growth [14,15]. The balancing of soil nutrients are required to identity the rice's good quality [16]. Soil is one of the main element in organisms living in which there are nutrients and water as food sources for plants [17].

The soil content consist of various mineral, nitrogen, and other organic compound [18]. The nitrogen (N) content in the soil is an essential nutrient for rice plants' growth. Nitrogen (N) cycle from the soil cause reduce soil fertility, plant growth [19] and environmental pollution [20,21] such as ammonia volatilization, nitrate leaching, and nitrous oxide emission [22] .

Hence, the controlling of N content in the soil must be considered for knowing the N content in the soil [23]. Three things cause the loss of nitrogen from the soil: The nitrogen in the lowland soils affects rice plants' vegetative growth [24,25]. The rainwater movement will cause soil activity[26,27], In order to, the soil quality is not monitored and detrimental rice farmers loss [28–30]. In increasing the farmer's welfare

* Corresponding author.
E-mail address: eyudhana@ee.uad.ac.id (A. Yudhana).

https://doi.org/10.1016/j.sbsr.2021.100435
Received 16 April 2021; Received in revised form 9 June 2021; Accepted 14 June 2021
Available online 18 June 2021

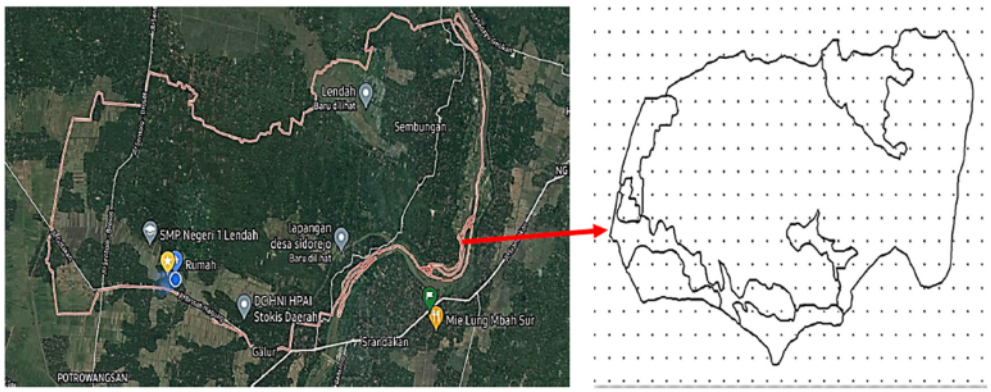

Fig. 1. Lendah sub-district in the Google Earth.

in their income, it is necessary to make the fertilizers efficient to save energy sources and increase rice production [31,32]. In this modern era, the rice farmers are still using the estimating method for knowing the soil quality and there is no tool used to determine the paddy land's quality [34]. In addition, mapping the paddy fields to identify nitrogen (N) content in the soil was required to the rice production [35,36].

There are many methods to conduct the mapping area in the agriculture field such as monitoring soil content by using remote sensing (RS) dan GIS has investigated by [37] to measure the water exploration in 3 zones: low potential zone, medium potential zone, and high potential zone. The developing of mapping tools has applied in Mekong Region, Vietnam by [38] thourght ArcGIs desktop 10.5 and digital model SRTM 30. ArcGIS software also can be applied for groundwater quality [39,40] to identify six soil textual classes (organic, coarse loamy, silt [41], clay, fine sand, and coarse sand) [42], soil erosion [43], and flood prediction [44–46].

In addition, GIS is an important tools to predict and mapping the spatial distribution of soil on the landscape [47]. The application of GIS can share the information regarding soil physicochemical parameter in precision farming to examine the soil properties such as nitrogen [48], sulfur [49], fluoride [50,51], potassium [52], and phosphorous [53]. ArcGIS can display the manipulate georeferenced information [54], store assemble [55], create georeferenced data, and generate multiple missing spatial data [56,57]. The procedure of GIS package is firstly choice the active zone [58] and the layers in the active zone as subdivided according the characteristics [59]. The study area was calculated by using spatial distribution maps and interpolating the data in each location [60,61].

In recently, The experiment in the mapping area of agriculture have used Machine Learning (ML) with high accuracy such as: Naïve Bayes [62,63], Support Vector Machine (SVM) [64,65], K Nearest Neighbors (KNN) [66,67], Bayesian Networks (BNs) [68,69], and Random Forest (RF) [70]. Application of Machine Learning is to predict the phenomena in future. The data classification in machine learning is the major important to get the high accuracy. In this experiment. Naïve Bayes was applied to predict the nitrogen soil level because Naïve Bayes have a high accuracy. In previous research, According to [71] that Naïve Bayes model was conducted to predict the genotype of maize with accuracy of 87%. Research from [72] have investigated the experiment abour the clarification of promotion images using Naïve Bayes with accuracy of 94%.

From the explanation above, the purpose of this experiment was applied for soil nitrogen mapping with a smart prototype using the TCS3200 sensor combined with Naive Bayes algorithm and GIS (Geographical information systems).. GIS-based mapping can be used as data for the farmers and the government in evaluating the possibility of soil nitrogen content in the rice fields. The Geographic Information

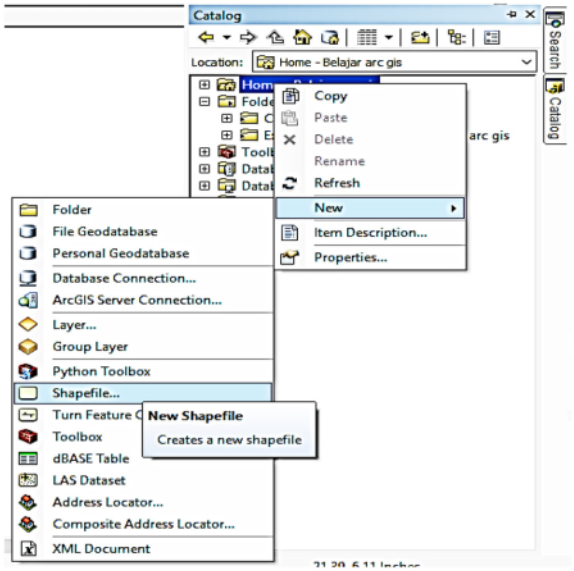

Fig. 2. Shapefile creation.

System (GIS) in mapping agricultural land was created to help develop the farmers' agricultural productivity and welfare.

2. Materials and methods

The design of the device, software design, and Arc GIS (*Geographic Information System)* are described below.

2.1. Study area

This experiment was conducted in Lendah sub-district, Kulonprogo, Indoneisa between longitudes 7° 38′42″-7° 59′3″ and lantitudes110° 1′37″- 110°16′26″. Lendah sub-distric was covered in 6 villages, namely Bumirejo Village, Wahuharjo Village, Ngetakrejo Village, Sidorejo Village and Gulurejo Village and including 62 hamlets, 115 RW, and 246 RT. The total of the population in lendah is 13,064 head of families. The rice field in Lendah is about 671.87 Ha that used for agriculture such as the cultivation of food crops grown in the rainy season and horticultural crops planted in the dry season. The general problem in this area is the

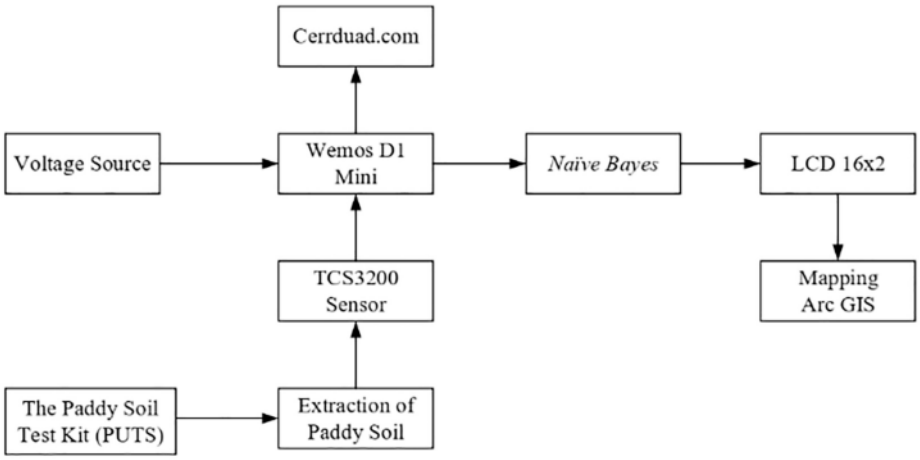

Fig. 3. System Block Diagram.

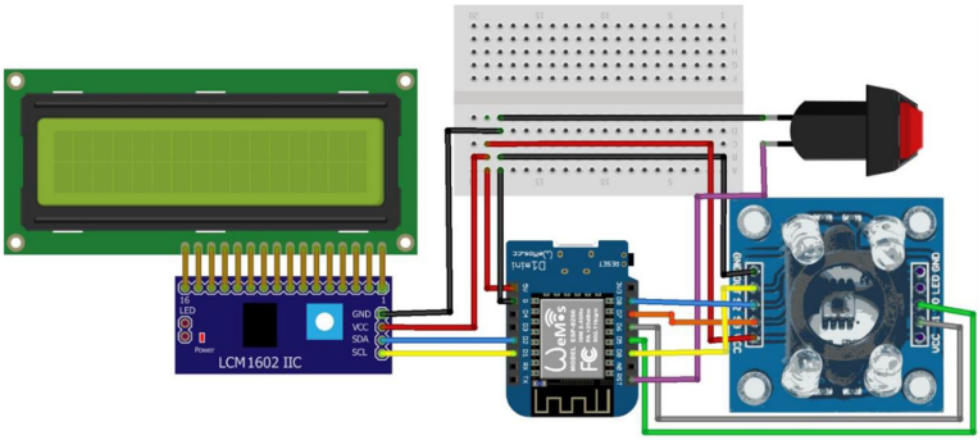

a) Diagram of the final assembly in electrical system

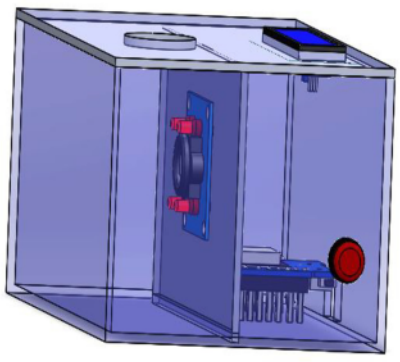

b) 3D Design of prototype

Fig. 4. Measurement system a) final assembly of electrical system, and b) 3D design of prototype.

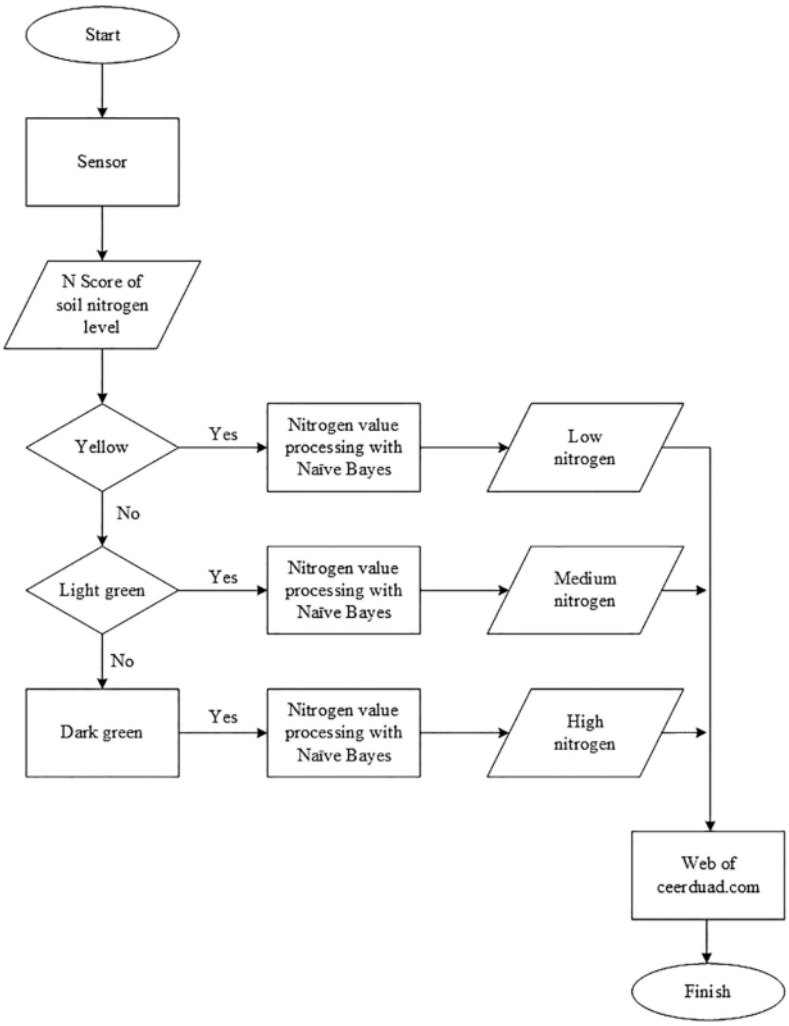

Fig. 5. Flowchart of the code algorithm for nitrogen soil mapping.

sociaty unknown the nitrogen soil level and unknown the information regarding the alternative technology to improve the rice production in real-time. It is recognized that information technology and supporting devices have a great effect on increasing agricultural production. The maps of Lendah sub-district was made based on the Lendah maps on google earth to get maps image based on the current situation or in real terms. The researcher took 20 soil samples in Lendah sub-district. From the results of these searches, Image maps of the Lendah location can be described in Fig. 1.

A map of Lendah sub-district was created by using shapefile. Fig. 2 shows the catalog to save the shapefile created. It has been created, click right, new and continue to shapefile, and select the polygon shape to create a map. Furthermore, the shapefile was appearance on the layers.

2.2. Design of the device

Fig. 3 shows the system block diagram. Hardware design to detect the N content in paddy soil was done by detecting RGB with the TCS3200 sensor which was installed by input the microcontroller. This research was conducted on a Wemos D1 Mini microcontroller because it has a compatible board at an affordable price [12].

Based on the system block diagram above, the sensor can read the N content detection with the result displayed in an RGB image then the sensor readings are processed by the Wemos D1 Mini displayed on the LCD and sent to the web server. From the LCD, it can be shown the mapping by using Arc GIS. The Arc GIS carry out the mapping. The block diagram in Fig. 3 can be implemented in Fig. 4.

Fig. 4 shows the design of a paddy field nitrogen meter. From design of the tools, the TCS3200 sensor must be placed in the hard case because the sensor readings color must be in a dark situation or light-proof. If there is a light inference, the sensor readings are less accurate.

2.3. Software design

Flow diagram of a measuring device for lowland soil nitrogen can be illustrated in Fig. 5. The sensor in this research was used the TCS3200. If there is an input of color from the soil extraction, the extracted paddy soil is read by the TCS3200 sensor then classified by Naïve Bayes. Finally, the results were displayed on the LCD screen and the data is sent to the website server.

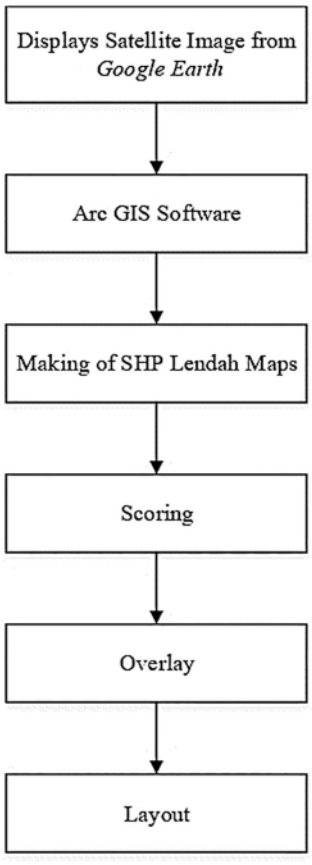

Fig. 6. Mapping design scheme.

2.3.1. Naïve Bayes classifier

Naïve Bayes Classifier is a classification method that came from the Bayes theorem to maximize the posterior possibility and also can be used to increasing the classification probability in variable and condition factors [73,74]. Thomas Bayes is an English scientist claiming the classification method using the probability and statistic method. The Bayes theorem known by the future predicts odds based on previous experiences [75,76].

The advantages of Naïve Bayes are that this method requires a little training data in determining the range of parameters used in the classification process because an independent variable took only the variant of a variable in a class needed to determine the classification without the whole of the covariance matrix [77]. According to [78] The Naïve Bayes classifier can be applied to approach the digital databases and incorporates methods including probability analysis, spatial pattern analysis, and interactive mapping. Naïve Bayes also has high accuracy and speed when using extensive data in the database to get small errors [79,80].

$$P(c/x) = \frac{P(x/c)P(c)}{P(x)} \quad (1)$$

Where, P(c/x) is the probability of categorized test data on the overall test data, P(x|c) represents lass.

Probability on all test data, P(c) is predictors prior probability, and P (x) is posterior probability.

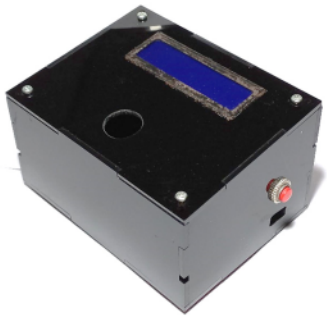

Fig. 7. A prototype of the paddy soil nitrogen meter.

2.4. Arc GIS

Geographic Information System (GIS) is a system that combines the text data (attributes) with the graphical data (spatial) objects that are linked geographically [81,82]. Arc GIS is a software developed by ESRI (Environment Science & Research Institute), which combines various GIS software functions. Types of software on the desktop Arc GIS include [83]:

- Arc View is used for fundamental spatial map analysis, can generate spatial data, and layered map design.
- Arc Map is used for map visualization, spatial data design, map editing, and map design.
- Arc Editor is used to manipulate shapefile data.
- Arc Info is used to manipulate data and data analysis.
- Arc Catalog is used to store GIS data and manage spatial data.

Geographic Information System is also devoted to data management with spatial information [84]. In addition, GIS can also link the data, organize the data, and perform data analysis to decide on the regional issues. In general, GIS is the earth's geographic information system used to provide 2D digital information from its analysis [85].

2.4.1. Mapping area with GIS

The scheme planning for the rice field is important to achieve the expected mapping results. Therefore, the mapping steps can be seen in Fig. 6 below.

The schematic in Fig. 6 begins with taking a map of the Lendah sub-district from Google Earth and inserting the map into the Arc GIS software. From the Lendah sub-district map image, a shapefile combined into one structure from the Lendah sub-district and a score is made for each polygon was created [86,87]. By the union map technique, it is combined and was produce the desired mapping. The display satellite image from google earth is to get maps image based on the current situation or in real terms. Arc GIS software is to mapping area and to obtain training data with 20 samples in Lendah, Indonesia. Making of SHP (Shapefile) is a step to save the maps image. Scoring is to calculated the soil nitrogen level based on the color parameter and the paddy soil nitrogen content. Overlay is applied to combine a shapefile into one structure. Layout is to described the mapping result of the paddy soil nitrogen.

3. Findings and discussions

3.1. Prototype of paddy soil nitrogen level meter

The prototype of the paddy soil nitrogen meter can be implemented in Fig. 7. The device must be tight and light-proof so that the TCS3200 sensor readings are not disturbed.

Table 1
The TCS3200 sensor test results and the paddy soil test kit (PUTS).

Testing	R	G	B	Device status	PUTS status	Soil code
1	158	142	116	Low	Medium	1
2	167	142	116	Medium	Medium	1
3	125	111	96	Low	Medium	2
4	136	121	104	Medium	Medium	2
5	168	140	110	High	High	3
6	163	142	112	High	High	3
7	125	111	96	Medium	Medium	4
8	136	121	104	Medium	Medium	4
9	157	143	116	Low	Low	5
10	148	140	115	Low	Low	5
11	145	133	112	Low	Low	6
12	147	133	113	Low	Low	6
13	127	116	96	Medium	Medium	7
14	140	123	103	Medium	Medium	7
15	148	136	112	Low	Low	8
16	142	136	110	Low	Low	8
17	158	143	112	Low	Low	9
18	166	149	119	Low	Low	9
19	118	113	96	Low	Low	10
20	127	121	103	Low	Low	10
21	132	126	98	Low	Low	11
22	145	131	106	Low	Low	11
23	138	121	101	High	High	12
24	145	128	108	High	High	12
25	137	123	101	Low	Low	13
26	144	128	104	Low	Low	13
27	148	145	118	Low	Low	14
28	158	148	118	Medium	Low	14
29	132	126	101	Low	Low	15
30	142	131	108	Low	Low	15
31	130	121	98	Medium	Medium	16
32	140	126	103	Medium	Medium	16
33	135	126	98	Low	Low	17
34	140	131	106	Low	Low	17
35	165	146	119	Medium	Medium	18
36	169	146	119	High	High	18
37	139	131	112	Low	Low	19
38	146	134	116	Low	Low	19
39	125	118	98	Low	Medium	20
40	137	124	103	Medium	Medium	20

3.2. Paddy soil testing by TCS3200 sensor

The paddy soil testing was tested by using TCS sensor to make the soil classification. The experiment result was described in Table 1 which the device status as the result from prototype and the Paddy Soil Test Kit (PUTS) as the standard data from government of Indonesia. The soil classification from prototype (Device status) was used to analysis of Naïve Bayes in this experiment. The TCS3200 sensor was carried out two readings for each oil sample.[27]

According to Table 1. It Shows the comparison of the testing TCS3200 sensor results and the testing results of the Paddy Field Test Kit (PUTS) that the results of TCS3200 sensor readings are not similar with the results of PUTS tests. So that the accuracy of the testing can be determined as follows:

$$\text{Accuracy} = \frac{\textit{Testing total–error}}{\textit{The number of testing}} \text{ x } 100\% \quad (2)$$

$$= 87.5\%$$

According to the eq 2, the accuracy level is 87.5%. This result was compared with previous research in the field of GIS mapping with the difference of applications and methods. The comparison detail can be described in Table 2. In addition, the accuracy in this study is higher than the previous research. The experimental result in this study is better than the previous research because this research made a prototype to check the N content of paddy soil using the TCS3200 sensor combined with Naive Bayes and GIS.The data from the systems can be show in the website server in which the design of prototype is simple and easy use.

Table 2
The comparison of accuracy between this study and previous study.

Studies	Methods	Application	Accuracy	Ref
Dedeoğlu and Dengiz, 2019	Hybrid system approach using analytic hierarchy process (AHP) and GI	Land suitability index	Accuracy of 83% and accuracy of NDVI (Normalized difference vegetation index) of 78%	[88]
Tehrany, Pradhan, and Jebur 2014	• Weigh-of Evidence WoE) model and SIG-SVM (Support vector machine model) • Standalone RBF (Radial basis function) and SVM	Flood susceptibility mapping	• Success rate accuracy of 84.67% and prediction rate of 84.28%. • Success rate accuracy of 86.47% and prediction rate of 81.27%	[89]
Elkhrachy, 2015	Satellite image and GIS Tools	Flash flood hazard mapping	Overall accuracy of 84.4% and Kappa coefficient of 82.5%	[90]
Akumu et al. 2015	GIS-Fuzzy logic based	Modeling soil texture	Overall accuracy of 79% and Kappa statistics of 70%	[42]
Msabi and Makonyo, 2021	GIS and multi-criteria decision analysis	Flood susceptibility mapping	Accuracy of 87.24%	[91]
Akumu, Baldwin, and Dennis, 2019	GIS based modeling	Soil moisture regime (SMR) Mapping	Overall accuracy of 65%	[23]
This study	GIS based	Nitrogen soil mapping	Accuracy of 87.5%	

3.3. Data delivery to the ceerduad.com web

The results data from the TCS3200 sensor readings was delivered to ceerduad.com website as the database to display the graph reading from TCS sensor in the form: Red, Green, Blue (RGB color). Data delivery to the can be seen in Fig. 8.

The website server in this research can be access by using email dan password to maintain security for users of this application. The display of website server can be seen in Fig. 8. website server features were used Indonesia language to make farmers understand and access this application easily. After login, the process forward in the website server can be seen in Fig. 8c. Click on Sensor Graph to see the graphical display of the TCS3200 sensor reading. Graph shows 3 colors including: Red, Green, and Blue (RGB color) that show the soil nitrogen condition in Lendah District. The data from the sensor was automatically stored and load in excel. The results of the TCS3200 sensor readings in excel can be shown in Table 3.

From the data in Table 2, it shows in real-time by using the Wemos D1 Mini microcontroller. The sending data was provided the form of RGB (Red, Green, and Blue) value data by the TCS3200 sensor readings and the sensor's nitrogen level status.

3.4. Determine of Naïve Bayes classifier

In this study, Naïve Bayes is used to explain the probability of nitrogen content in the soil based on 3 categories, namely low, medium, and high. The amount of analysis data is as many as 40 classifications and divided into 22 classes of low, 13 classes of medium, and 5 classes of high. Data classification of soil can be seen in Table 1. The nitrogen probabilities (low, medium, and high) are the probability of the total

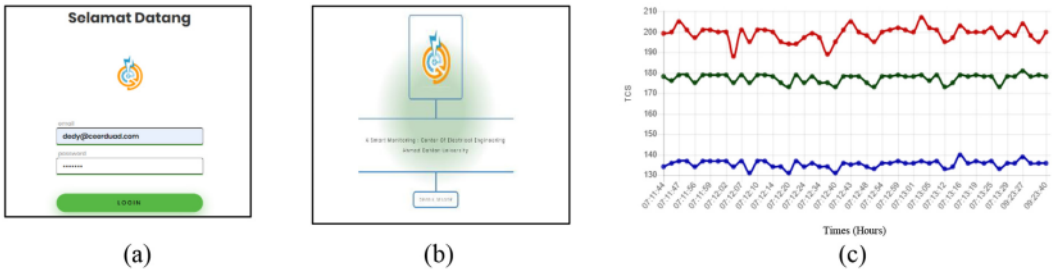

Fig. 8. The step of data delivery: (a)The ceerduad.com Web Login Page; (b) The Display of Sensor Graphic; (c) The Sensor Graph on ceerduad.com Web.

Table 3
The TCS3200 data backed up on the website server.

No	Red	Green	Blue	Status	Hours	Date
1	191	223	183	Medium	12:13:42	2020-04-21
2	186	216	181	Medium	12:13:44	2020-04-21
3	189	221	183	Medium	12:13:45	2020-04-21
4	191	222	183	Medium	12:13:48	2020-04-21
5	176	223	221	Medium	12:13:49	2020-04-21
6	189	218	181	Medium	12:13:54	2020-04-21
7	189	221	183	Medium	12:13:57	2020-04-21
8	194	226	188	Medium	12:14:00	2020-04-21
9	196	228	201	Medium	12:14:01	2020-04-21
10	136	111	123	Medium	12:14:03	2020-04-21

Table 4
Red odds.

Red						
Range of value	Low	Medium	High	P (rre)	P (rse)	P (rti)
44 -86	0	0	0	0/23	0/14	0/3
87 - 129	2	4	0	2/23	4/13	0/3
130 - 172	20	10	4	20/23	10/13	4/4
173 - 255	0	0	0	0/23	0/14	0/3

Table 5
Green odds.

Green						
Range of value	Low	Medium	High	P (gre)	P (gse)	P (gti)
44 - 86 &	0	0	0	0/23	0/14	0/3
87 - 129	7	10	2	7/23	10/13	2/4
130 -172	15	4	2	15/23	4/13	2/4
173 - 255	0	0	0	0/23	0/14	0/3

Table 6
Blue odds.

Blue						
Range of value	Low	Medium	High	P (bre)	P (bse)	P (bti)
44 - 86	0	0	0	0/23	0/14	0/3
87 - 129	22	14	4	22/23	14/13	4/4
130 - 172	0	0	0	0/23	0/14	0/3
173 - 255	0	0	0	0/23	0/14	0/3

readings of the TCS3200 sensor and divided by the whole data with the results are 0.55 of low, 0.325 of medium, and 0.125 of high. The detail calculations are:

a. Low nitrogen probabilities
$P(c(low)) = 22/40 = 0.55$
b. Medium nitrogen probabilities
$P(c(medium)) = 13/40 = 0.325$
c. High nitrogen probabilities
$P(c(high)) = 5/40 = 0.125$.

Then, the classification result of RGB value was performed in Tables 4, 5, and 6.

Table. 4 shows four classifications of opportunities for reading Red with different values of ranges. Red readings are at low (P(rre)), medium (P(rse)), and high (P(rti)).

Table 5 shows four classifications of opportunities for reading Green with different values of ranges. Green reading at low (P(gre)), medium (P(gse)), and high (P(gti)).

Table 6 shows four classifications of opportunities for reading Blue with different values of ranges. Blue readings are at low (P(bre)), medium (P(bse)), and high (P(bti)). The RGB value from the TCS3200 sensor is $X = \{R = 118; G = 125; B = 145\}$, then the nitrogen content of paddy soil was calculated by using Naïve Bayes Algorithm and using Eq 1 as follows:

a. Determine P(c), the low, medium, and high probability of the sensor reading data and the amount of data

$P\ (re) = 23/40.$
$P\ (se) = 13/40.$
$P\ (ti) = 5/40$

b. Determine P(x/c), the low, medium, and high of the RGB color Table 4, 5 and 6,

- Low odds

$P(rre) = \frac{20}{23}; P(gre) = \frac{15}{23}; P(bre) = \frac{22}{23}$

- Medium odds

$P(rse) = \frac{10}{13}; P(gse) = \frac{10}{13}; P(bse) = \frac{14}{13}$

- High odds

$P(rti) = \frac{4}{4}; P(gti) = \frac{2}{4}; P(bti) = \frac{4}{4}$

c. Determine P(x|c)P(c)

- Low

$P(x|re)\ P(R) = 0.27$

- Medium

$P(x|se)P(S) = 0.20$

Table 7
Color classification of nitrogen levels.

	Color	Nitrogen content	Score
1		Low	1
2		Medium	2
3		High	3

Table 8
The N score of the soil nitrogen levels.

FID	Shape	Soil sample	N content	N score
2	Polygon	1	Medium	2
1	Polygon	2	Medium	2
0	Polygon	3	High	3
3	Polygon	4	Medium	2
4	Polygon	5	Low	1
5	Polygon	6	Low	1
6	Polygon	7	Medium	2
7	Polygon	8	Low	1
8	Polygon	9	Low	1
9	Polygon	10	Low	1
10	Polygon	11	Low	1
11	Polygon	12	High	3
12	Polygon	13	Low	1
13	Polygon	14	Low	1
14	Polygon	15	Low	1
15	Polygon	16	Medium	2
16	Polygon	17	Low	1
17	Polygon	18	Medium	2
18	Polygon	19	Low	1
19	Polygon	20	Medium	2

- High

  P(x|ti)P(T) = 0.05

d. Calculate the set value of X on all data

  P(x) = 0.45

e. Identify the odds of the low, medium, and high nitrogen levels.

- Low

  P(re|x) = 0.60

- Medium

  P(se|x) = 0.40

- High

  P(ti|x) = 0.11.

Therefore, the results of the calculation with *naïve bayes* can be concluded if P(re|x) > P(se|x) dan P(re|x) > P(ti|x). Then the nitrogen content was category low. The same procedures were repeated to define the medium and high level.

This result was compared with previous research from [92] by using Mahalanobis Distance Analysis (MD) with the RGB values are 213 of R, 111 of G, and 56 of B. MD analysis from [92] was found 3 variations: principle component 1, 2, and 3 (PC1, PC2, and PC3) with the result −5.72 to 3.57, − 3.01 to 2.36, and − 0.93 to 1.08, respectively.

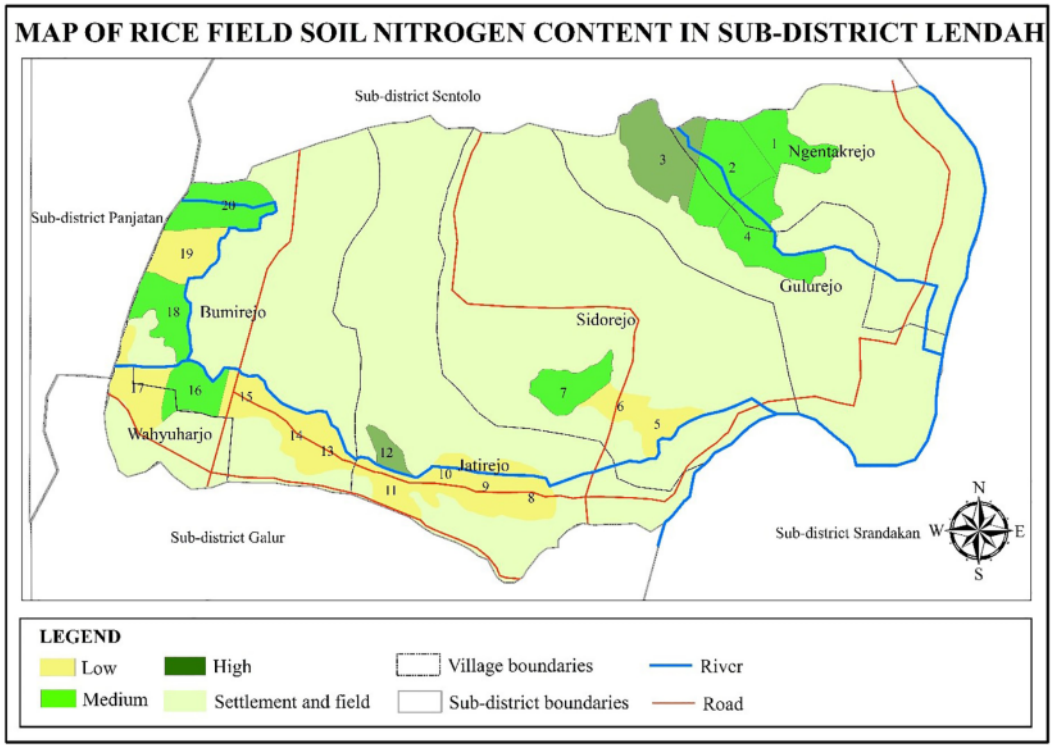

Fig. 9. Map of the soil nitrogen content of the Lendah district.

3.5. Nitrogen soil mapping by Arc GIS

The data soil was performed in the polygon with 20 samples. The mapping area was made based on the results of nitrogen measurements of paddy soil by grouping several levels of nitrogen content. According to the Agricultural R & D Agency, the nitrogen measurement results are divided into three; low, medium, and high.. Therefore, the nitrogen content parameter can be made into a paddy soil nitrogen content grouping which can be seen in Table 7.

From the nitrogen measurements based on the colors, there are three levels of nitrogen content. Therefore, the Scoring for the color's parameter and the paddy soil nitrogen content in Lendah sub-district can be illustrated in Table 8.

After collecting the paddy soil nitrogen content, the results in 20 points/place of the soil sampling which the mapping of lowland soil in the Lendah sub-district can be implemented. Based on the attribute data Table 8, the map of lowland soil nitrogen content in Lendah district can be seen in Fig. 9.

From the mapping results of the paddy soil nitrogen in Lendah district, there are three levels of nitrogen levels. Paddy soil nitrogen with a yellow color (score = 1) is described as a low nitrogen level with the percentage of 55%. The light green color(score = 2) reflects moderate nitrogen levels with the rate of 35%. Meanwhile, the dark green color (score = 3) is described as high nitrogen content with the percentage of 10% from the number of samples measured nitrogen content. The experiment result of nitrogen soil mapping was clarified in four levels: low of 55%, medium of 35%, and high of 10% from the number of samples. This result was relevant to the previous research in the field of soil erosion and flood hazard [93], soil protection function of forest ecosystems [94], evaluation of land suitability [94,95,96], and soil fertility index [97].

4. Conclusion

A paddy field nitrogen levels by using the TCS3200 sensor and the Wemos D1 Mini microcontroller has been proven to measure rice fields' nitrogen content. The data of the sensors were succesfully sent to the web ceerduad.com . The implementation of GIS for nitrogen soil mapping was succesfully developed with accuracy of the system is 87.5%. The data classification of soil nitrogen in this research was succesfully by using Naive Bayes. Mapping of the paddy soil nitrogen Lendah sub-district with Geographic Information System (GIS) was successfully created to perform the analysis and action quickly in the rice field area with low, medium, or high nitrogen levels.

Funding

This research was supported by Institute of Research and Community Services (LPPM) Universitas Ahmad Dahlan, Yogyakarta, Indonesia.

Declaration of Competing Interest

The authors have stated no conflict of interest.

Acknowledgments

We would like to show our gratitude to Dr. Sunardi, M.T., the Dean of Industrial Technology of Universitas Ahmad Dahlan and Nuryono Satya Widodo, M.Eng. the Head of Electrical Department of Universitas Ahmad Dahlan for sharing their pearls of wisdom with us during the course of this research.

References

[1] X. Jia, B. Hu, B.P. Marchant, L. Zhou, Z. Shi, Y. Zhu, A methodological framework for identifying potential sources of soil heavy metal pollution based on machine learning: a case study in the Yangtze Delta, China, Environ. Pollut. 250 (2019) 601–609, https://doi.org/10.1016/j.envpol.2019.04.047.

[2] B.P. Statistics Indonesia. Harvasted Area and Rice Production in Indonesia, I st eddit, Central Bureau of Statistics, Jakarta, Indonesia, 2018, pp. 1–25, 05110.1806.

[3] W. Masiza, J.G. Chirima, H. Hamandawana, R. Pillay, Enhanced mapping of a smallholder crop farming landscape through image fusion and model stacking, Int. J. Remote Sens. 41 (22) (2020) 8736–8753, https://doi.org/10.1080/01431161.2020.1783017.

[4] J.B. Nsengiyumva, R. Valentino, Predicting landslide susceptibility and risks using GIS-based machine learning simulations, case of upper Nyabarongo catchment, Geomatics, Nat. Hazards Risk 11 (1) (2020) 1250–1277, https://doi.org/10.1080/19475705.2020.1785555.

[5] P.R. Yoon, J.Y. Choi, Effects of shift in growing season due to climate change on rice yield and crop water requirements, Paddy Water Environ. 18 (2) (2020) 291–307, https://doi.org/10.1007/s10333-019-00782-7.

[6] M. Avand, H. Moradi, M.R. Lasboyee, Using machine learning models, remote sensing, and GIS to investigate the effects of changing climates and land uses on flood probability, J. Hydrol. 595 (2021), https://doi.org/10.1016/j.jhydrol.2020.125663.

[7] T. Takama, E. Aldrian, Climate Change Vulnerability to Rice Paddy Production in Bali, Indonesia, *Springer*, 2014, https://doi.org/10.1007/978-3-642-40455-9 no. January.

[8] N.T. Chung, A. Jintrawet, P. Promburom, Impacts of seasonal climate variability on rice production in the central highlands of Vietnam, Agric. Agric. Sci. Procedia 5 (2015) 83–88, https://doi.org/10.1016/j.aaspro.2015.08.012.

[9] A. Yudhana, A. C Kusuma, Water quality monitoring at paddies farming based on android, IOP Conference Series: Materials Science and Engineering 403 (1) (2018), 012042, https://doi.org/10.1088/1757-899X/403/1/012042.

[10] D.G.C. Kirono, J.R.A. Butler, J.L. McGregor, A. Ripaldi, J. Katzfey, K. Nguyen, Historical and future seasonal rainfall variability in Nusa Tenggara Barat Province, Indonesia: implications for the agriculture and water sectors, Clim. Risk Manag. 12 (2016) 45–58, https://doi.org/10.1016/j.crm.2015.12.002.

[11] R.L. Naylor, D.S. Battisti, D.J. Vimont, W.P. Falcon, M.B. Burke, Assessing risks of climate variability and climate change for Indonesian rice agriculture, Proc. Natl. Acad. Sci. U. S. A. 104 (19) (2007) 7752–7757, https://doi.org/10.1073/pnas.0701825104.

[12] T. Yuliawan, I. Handoko, The effect of temperature rise to rice crop yield in Indonesia uses shierary rice model with geographical information system (GIS) feature, Procedia Environ. Sci. 33 (2016) 214–220, https://doi.org/10.1016/j.proenv.2016.03.072.

[13] A.C.R. Lima, W.B. Hoogmoed, L. Brussaard, F. Sacco Dos Anjos, Farmers' assessment of soil quality in rice production systems, NJAS - Wageningen J. Life Sci. 58 (1–2) (2011) 31–38, https://doi.org/10.1016/j.njas.2010.08.002.

[14] B.D. Khaki, N. Honarjoo, N. Davatgar, A. Jalalian, H.T. Golsefidi, Assessment of two soil fertility indexes to evaluate paddy fields for rice cultivation, Sustain. 9 (8) (2017) 1–13, https://doi.org/10.3390/su9081299.

[15] M. Pulido Moncada, D. Gabriels, D. Lobo, J.C. Rey, W.M. Cornelis, Visual field assessment of soil structural quality in tropical soils, Soil Tillage Res. 139 (2014) 8–18, https://doi.org/10.1016/j.still.2014.01.002.

[16] T.S. Sukitprapanon, M. Jantamenchai, D. Tulaphitak, P. Vityakon, Nutrient composition of diverse organic residues and their long-term effects on available nutrients in a tropical sandy soil, Heliyon 6 (11) (2020), e05601, https://doi.org/10.1016/j.heliyon.2020.e05601.

[17] A. Yudhana, Z. Salsabila, H.K Dewi, H. Yuliansyah, D.D Fairus, Moisture monitoring of rice fields in Jogotirto, Sleman using internet of things, International Conference of Science and Technology for Internet of Things 3 (2) (2018), https://doi.org/10.4108/eai.20-9-2019.2292093.

[18] Z. Shirvani, A holistic analysis for landslide susceptibility mapping applying geographic object-based random forest: a comparison between protected and non-protected forests, Remote Sens. 12 (3) (2020), https://doi.org/10.3390/rs12030434.

[19] C.W. Liu, Y. Sung, B.C. Chen, H.Y. Lai, Effects of nitrogen fertilizers on the growth and nitrate content of lettuce (Lactuca sativa L.), Int. J. Environ. Res. Public Health 11 (4) (2014) 4427–4440, https://doi.org/10.3390/ijerph110404427.

[20] F.S. Gilliam, J.H. Billmyer, C.A. Walter, W.T. Peterjohn, Effects of excess nitrogen on biogeochemistry of a temperate hardwood forest: evidence of nutrient redistribution by a forest understory species, Atmos. Environ. 146 (2016) 261–270, https://doi.org/10.1016/j.atmosenv.2016.04.007.

[21] A. Yudhana, Y.D. Andriliana, S.A. Akbar, Sunardi, S. Mukhopadhyay, I.R. Karas, Monitoring of rainfall level obrometer observatory (Obs) type using android sharp GP2Y0A41SKOF sensor, International Journal of Advanced Computer Science and Applications 10 (11) (2019) 360–364, https://doi.org/10.14569/ijacsa.2019.0101150.

[22] K.C. Cameron, H.J. Di, J.L. Moir, Nitrogen losses from the soil/plant system: a review, Ann. Appl. Biol. 162 (2) (2013) 145–173, https://doi.org/10.1111/aab.12014.

[23] C.E. Akumu, K. Baldwin, S. Dennis, GIS-based modeling of forest soil moisture regime classes: using Rinker Lake in Northwestern Ontario, Canada as a case study, Geoderma 351 (2019) 25–35, https://doi.org/10.1016/j.geoderma.2019.05.014.

[24] B.M. Moro, I.R. Nuhu, E. Ato, B. Nathanial, Effect of nitrogen rates on the growth and yield of three rice (*Oryza sativa* L .) varieties in rain-fed lowland in the forest agro-ecological zone of Ghana, Int. J. Agric. Sci. ISSN 5 (7) (2015) 878–885.

[25] A. Leon, K. Kohyama, Estimating nitrogen and phosphorus losses from lowland paddy rice fields during cropping seasons and its application for life cycle assessment, J. Clean. Prod. 164 (2017) 963–979, https://doi.org/10.1016/j.jclepro.2017.06.116.

[26] T.I. Jang, H.K. Kim, C.H. Seong, E.J. Lee, S.W. Park, Assessing nutrient losses of reclaimed wastewater irrigation in paddy fields for sustainable agriculture, Agric. Water Manag. 104 (2012) 235–243, https://doi.org/10.1016/j.agwat.2011.12.022.

[27] Y. He, Z. Jianyun, Y. Shihong, H. Dalin, X. Junzeng, Effect of controlled drainage on nitrogen losses from controlled irrigation paddy fields through subsurface drainage and ammonia volatilization after fertilization, Agric. Water Manag. 221 (2019) 231–237, https://doi.org/10.1016/j.agwat.2019.03.043. January 2018.

[28] A. Yudhana, A.C. Kusuma, Water quality monitoring at paddies farming based on android, IOP Conf. Ser. Mater. Sci. Eng. 403 (1) (2018), https://doi.org/10.1088/1757-899X/403/1/012042.

[29] K. Jha, A. Doshi, P. Patel, M. Shah, A comprehensive review on automation in agriculture using artificial intelligence, Artif. Intell. Agric. 2 (2019) 1–12, https://doi.org/10.1016/j.aiia.2019.05.004.

[30] D. Devapal, Smart agro farm solar powered soil and weather monitoring system for farmers, Mater. Today Proc. 24 (2019) 1843–1854, https://doi.org/10.1016/j.matpr.2020.03.609.

[31] A.B. Tarigan, Marheni, J. Ginting, Application of fertilizer type and dosage toward brown planthopper (*Nilaparvata lugens* Stall.) attack level on several paddy (*Oryza sativa* L.) varieties, IOP Conf. Ser. Earth Environ. Sci. 260 (1) (2019), https://doi.org/10.1088/1755-1315/260/1/012179.

[32] B.W. Hariyadi, F. Nizak, I.R. Nurmalasari, Effect of Dose And Time of Npk Fertilizer Application on The Growth And Yield of Tomato Plants (Lycopersicum Esculentum Mill), Agric. 2 (2) (2019) 101–111 [Online]. Available: https://eprints.unmerbaya.ac.id/id/eprint/208/.

[34] D. Manikandan, A.M. Skl, T. Sethukarasi, Agro-gain - an absolute agriculture by sensing and data-driven through iot platform, Procedia. Comput. Sci. 172 (2019) (2020) 534–539, https://doi.org/10.1016/j.procs.2020.05.065.

[35] J. Dong, X. Xiao, Evolution of regional to global paddy rice mapping methods: a review, ISPRS J. Photogramm. Remote Sens. 119 (2016) 214–227, https://doi.org/10.1016/j.isprsjprs.2016.05.010.

[36] X. Jiang, B. Zou, H. Feng, J. Tang, Y. Tu, X. Zhao, Spatial distribution mapping of Hg contamination in subclass agricultural soils using GIS enhanced multiple linear regression, J. Geochem. Explor. 196 (2019) 1–7, https://doi.org/10.1016/j.gexplo.2018.10.002.

[37] O.A. Adeyeye, E.A. Ikpokonte, S.A. Arabi, GIS-based groundwater potential mapping within Dengi area, North Central Nigeria, Egypt. J. Remote Sens. Sp. Sci. 22 (2) (2019) 175–181, https://doi.org/10.1016/j.ejrs.2018.04.003.

[38] A. Aekakkararungroj, et al., A publicly available GIS-based web platform for reservoir inundation mapping in the lower Mekong region, Environ. Model. Softw. 123 (2020) 104552, https://doi.org/10.1016/j.envsoft.2019.104552.

[39] P. Yariyan, et al., Flood susceptibility mapping using an improved analytic network process with statistical models, Geomatics, Nat. Hazards Risk 11 (1) (2020) 2282–2314, https://doi.org/10.1080/19475705.2020.1836036.

[40] X. Tang, Y. Shu, Y. Lian, Y. Zhao, Y. Fu, A spatial assessment of urban waterlogging risk based on a weighted Naïve Bayes classifier, Sci. Total Environ. 630 (2018) 264–274, https://doi.org/10.1016/j.scitotenv.2018.02.172.

[41] G. Zhou, R. Zhang, D. Zhang, Manifold learning co-location decision tree for remotely sensed imagery classification, Remote Sens. 8 (10) (2016), https://doi.org/10.3390/rs8100855.

[42] C.E. Akumu, et al., GIS-fuzzy logic based approach in modeling soil texture: using parts of the Clay Belt and Hornepayne region in Ontario Canada as a case study, Geoderma 239–240 (2015) 13–24, https://doi.org/10.1016/j.geoderma.2014.09.021.

[43] B. Aslam, A. Maqsoom, W. Salah Alaloul, M. Ali Musarat, T. Jabbar, A. Zafar, Soil erosion susceptibility mapping using a GIS-based multi-criteria decision approach: case of district Chitral, Pakistan, Ain Shams Eng. J (2020), https://doi.org/10.1016/j.asej.2020.09.015.

[44] C. Di Salvo, F. Pennica, G. Ciotoli, G.P. Cavinato, A GIS-based procedure for preliminary mapping of pluvial flood risk at metropolitan scale, Environ. Model. Softw. 107 (2018) 64–84, https://doi.org/10.1016/j.envsoft.2018.05.020.

[45] V.-H. Nhu, et al., Mapping of groundwater spring potential in karst aquifer system using novel ensemble bivariate and multivariate models, Water (Switzerland) 12 (4) (2020) 1–25, https://doi.org/10.3390/W12040985.

[46] U. Sur, P. Singh, S.R. Meena, Landslide susceptibility assessment in a lesser Himalayan road corridor (India) applying fuzzy AHP technique and earth-observation data, Geomatics, Nat. Hazards Risk 11 (1) (2020) 2176–2209, https://doi.org/10.1080/19475705.2020.1836038.

[47] F. Baker, C. Smith, A GIS and object based image analysis approach to mapping the greenspace composition of domestic gardens in Leicester, UK, Landsc. Urban Plan. 183 (2019) 133–146, https://doi.org/10.1016/j.landurbplan.2018.12.002.

[48] S. Ettazarini, M. El Jakani, Mapping of groundwater potentiality in fractured aquifers using remote sensing and GIS techniques: the case of Tafraoute region, Morocco, Environ. Earth Sci. 79 (5) (2020), https://doi.org/10.1007/s12665-020-8848-1.

[49] J. Liu, K.M. Kamarudin, Y. Liu, J. Zou, Developing pandemic prevention and control by anp-qfd approach: a case study on urban furniture design in China communities, Int. J. Environ. Res. Public Health 18 (5) (2021) 1–26, https://doi.org/10.3390/ijerph18052653.

[50] K. Chaudhary, P.K. Saraswat, S. Khan, Improvement in fluoride remediation technology using GIS based mapping of fluoride contaminated groundwater and microbe assisted phytoremediation, Ecotoxicol. Environ. Saf. 168 (2019) 164–176, https://doi.org/10.1016/j.ecoenv.2018.10.007.

[51] D. Karunanidhi, P. Aravinthasamy, M. Deepali, T. Subramani, K. Shankar, Groundwater pollution and human health risks in an industrialized region of Southern India: impacts of the COVID-19 lockdown and the monsoon seasonal cycles, Arch. Environ. Contam. Toxicol. 80 (1) (2021) 259–276, https://doi.org/10.1007/s00244-020-00797-w.

[52] S. Elidrissi, F.E. Omdi, A. El Azhari, N. Fagel, L. Daoudi, New application of GIS and statistical analysis in mapping the distribution of quaternary calcrete (Tensift Al Haouz area, Central Morocco), CATENA 188 (2020) 104419, https://doi.org/10.1016/j.catena.2019.104419.

[53] H.U. Leena, B.G. Premasudha, S. Panneerselvam, P.K. Basavaraja, Pedometric mapping for soil fertility management – a case study, J. Saudi Soc. Agric. Sci. 20 (2) (2021) 128–135, https://doi.org/10.1016/j.jssas.2020.12.008.

[54] K. Koenig, B. Höfle, M. Hämmerle, T. Jarmer, B. Siegmann, H. Lilienthal, Comparative classification analysis of post-harvest growth detection from terrestrial LiDAR point clouds in precision agriculture, ISPRS J. Photogramm. Remote Sens. 104 (2015) 112–125, https://doi.org/10.1016/j.isprsjprs.2015.03.003.

[55] L. Kang, Street architecture landscape design based on wireless internet of things and GIS system, Microprocess. Microsyst. 80 (2021) 103362, https://doi.org/10.1016/j.micpro.2020.103362.

[56] R. Wu, X. Zhang, Q. Yuan, X. Lu, Landscape design of urban theme park based on GIS system and internet of things, Microprocess. Microsyst. (2020) 103396, https://doi.org/10.1016/j.micpro.2020.103396.

[57] D. Al-Shammari, I. Fuentes, B.M. Whelan, P. Filippi, T.F.A. Bishop, Mapping of cotton fields within-season using phenology-based metrics derived from a time series of landsat imagery, Remote Sens. 12 (18) (2020), https://doi.org/10.3390/RS12183038.

[58] A. Arabameri, B. Paradha, K. Rezaei, GIS-based landslide susceptibility mapping using numerical risk factor bivariate model and its ensemble with linear multivariate regression and boosted regression tree algorithms, Model. Earth Syst. Environ. 16 (3) (2019) 595–618, https://doi.org/10.1007/s11629-018-5168-y.

[59] W. Zhou, D. Alderton, S. A. B. T.-E. of G. Second E. Elias (Eds.), GIS for Earth Sciences, Academic Press, Oxford, 2021, pp. 281–293.

[60] V.-H. Dang, N.-D. Hoang, L.-M.-D. Nguyen, D.T. Bui, P. Samui, A novel GIS-Based random forest machine algorithm for the spatial prediction of shallow landslide susceptibility, Forests 11 (1) (2020), https://doi.org/10.3390/f11010118.

[61] M.S. Tehrany, L. Kumar, F. Shabani, A novel GIS-based ensemble technique for flood susceptibility mapping using evidential belief function and support vector machine: Brisbane, Australia, PeerJ 10 (2019) 2019, https://doi.org/10.7717/peerj.7653.

[62] A. Arabameri, W. Chen, T. Blaschke, J.P. Tiefenbacher, B. Pradhan, D.T. Bui, Gully head-cut distribution modeling using machine learning methods-a case study of N. W. Iran, Water (Switzerland) 12 (1) (2020), https://doi.org/10.3390/w12010016.

[63] R.N. Rachmawati, N.H. Pusponegoro, Spatial Bayes analysis on cases of malnutrition in East Nusa Tenggara, Indonesia, Procedia. Comput. Sci. 179 (2020) (2021) 337–343, https://doi.org/10.1016/j.procs.2021.01.014.

[64] G. Prabakaran, D. Vaithiyanathan, M. Ganesan, FPGA based effective agriculture productivity prediction system using fuzzy support vector machine, Math. Comput. Simul. 185 (2021) 1–16, https://doi.org/10.1016/j.matcom.2020.12.011.

[65] M. Ahmadlou, et al., Flood susceptibility mapping and assessment using a novel deep learning model combining multilayer perceptron and autoencoder neural networks, J. Flood Risk Manag 14 (1) (2021), https://doi.org/10.1111/jfr3.12683.

[66] D. Tien Bui, et al., A new intelligence approach based on GIS-based multivariate adaptive regression splines and metaheuristic optimization for predicting flash flood susceptible areas at high-frequency tropical typhoon area, J. Hydrol. 575 (2019) 314–326, https://doi.org/10.1016/j.jhydrol.2019.05.046.

[67] A. Motevalli, S.A. Naghibi, H. Hashemi, R. Berndtsson, B. Pradhan, V. Gholami, Inverse method using boosted regression tree and k-nearest neighbor to quantify effects of point and non-point source nitrate pollution in groundwater, J. Clean. Prod. 228 (2019) 1248–1263, https://doi.org/10.1016/j.jclepro.2019.04.293.

[68] P.A. Aguilera, A. Fernández, R. Fernández, R. Rumí, A. Salmerón, Bayesian networks in environmental modelling, Environ. Model. Softw. 26 (12) (2011) 1376–1388, https://doi.org/10.1016/j.envsoft.2011.06.004.

[69] P.A. Aguilera, A. Fernández, F. Reche, R. Rumí, Hybrid Bayesian network classifiers: application to species distribution models, Environ. Model. Softw. 25 (12) (2010) 1630–1639, https://doi.org/10.1016/j.envsoft.2010.04.016.

[70] H.R. Pourghasemi, et al., Assessment of urban infrastructures exposed to flood using susceptibility map and Google earth engine, IEEE J. Sel. Top. Appl. Earth Obs. Remote Sens. 14 (2021) 1923–1937, https://doi.org/10.1109/JSTARS.2020.3045278.

[71] D. Seka, B.S. Bonny, A.N. Yoboué, S.R. Sié, B.A. Adopo-Gourène, Identification of maize (Zea mays L.) progeny genotypes based on two probabilistic approaches: logistic regression and naïve Bayes, Artif. Intell. Agric. 1 (2019) 9–13, https://doi.org/10.1016/j.aiia.2019.03.001.

[72] P. Hubert, R. Sudaryono Phoenix, D. Suhartono, Classifying promotion images using optical character recognition and Naïve Bayes classifier, Procedia. Comput. Sci. 179 (2020) (2021) 498–506, https://doi.org/10.1016/j.procs.2021.01.033.

[73] D.T. Bui, et al., Landslide detection and susceptibility mapping by AIRSAR data using support vector machine and index of entropy models in Cameron Highlands, Malaysia, Remote Sens. 10 (10) (2018), https://doi.org/10.3390/rs10101527.

[74] B.T. Pham, D. Tien Bui, H.R. Pourghasemi, P. Indra, M.B. Dholakia, Landslide susceptibility assesssment in the Uttarakhand area (India) using GIS: a comparison study of prediction capability of naïve bayes, multilayer perceptron neural networks, and functional trees methods, Theor. Appl. Climatol. 128 (1–2) (2017) 255–273, https://doi.org/10.1007/s00704-015-1702-9.

[75] R. Priya, D. Ramesh, E. Khosla, Crop Prediction on the Region Belts of India: A Naïve Bayes MapReduce Precision Agricultural Model, 2018 *Int. Conf. Adv. Comput. Commun. Informatics, ICACCI 2018* (2018) 99–104, https://doi.org/10.1109/ICACCI.2018.8554948.

[76] R. Jahan, Applying Naive Bayes classification technique for classification of improved agricultural land soils, Int. J. Res. Appl. Sci. Eng. Technol 6 (5) (2018) 189–193, https://doi.org/10.22214/ijraset.2018.5030.
[77] W. Paas, J.C.J. Groot, Creating adaptive farm typologies using naive Bayesian classification, Inf. Process. Agric. 4 (3) (2017) 220–227, https://doi.org/10.1016/j.inpa.2017.05.005.
[78] A. Kadirhodjaev, P.R. Kadavi, C.-W. Lee, S. Lee, Analysis of the relationships between topographic factors and landslide occurrence and their application to landslide susceptibility mapping: a case study of Mingchukur, Uzbekistan, Geosci. J. 22 (6) (2018) 1053–1067, https://doi.org/10.1007/s12303-018-0052-x.
[79] T. Setiadi, F. Noviyanto, H. Hardianto, A. Tarmuji, A. Fadlil, M. Wibowo, Implementation of naïve bayes method in food crops planting recommendation, Int. J. Sci. Technol. Res. 9 (2) (2020) 4750–4755.
[80] H. Zhang, Z.X. Cao, M. Li, Y.Z. Li, C. Peng, Novel naïve Bayes classification models for predicting the carcinogenicity of chemicals, Food Chem. Toxicol. 97 (2016) 141–149, https://doi.org/10.1016/j.fct.2016.09.005.
[81] M. Ismail, M.K. Abdel Ghaffar, M.A. Azzam, GIS application to identify the potential for certain irrigated agriculture uses on some soils in Western Desert, Egypt, Egypt. J. Remote Sens. Sp. Sci. 15 (1) (2012) 39–51, https://doi.org/10.1016/j.ejrs.2012.03.001.
[82] M.N. Gebeyehu, Remote sensing and GIS application in Agriculture and Natural Resource Management, Int. J. Environ. Sci. Nat. Resour 19 (2) (2019), https://doi.org/10.19080/ijesnr.2019.19.556009.
[83] R. Sharma, S.S. Kamble, A. Gunasekaran, Big GIS analytics framework for agriculture supply chains: A literature review identifying the current trends and future perspectives, Comput. Electron. Agric. 155 (2018) 103–120, https://doi.org/10.1016/j.compag.2018.10.001, no. October.
[84] M.A. Hossain Bhuiyan, S. Chandra Karmaker, M. Bodrud-Doza, M.A. Rakib, B. B. Saha, Enrichment, sources and ecological risk mapping of heavy metals in agricultural soils of Dhaka district employing SOM, PMF and GIS methods, Chemosphere 263 (2021) 128339, https://doi.org/10.1016/j.chemosphere.2020.128339.
[85] U. Atila, I.R. Karas, A. Abdul-Rahman, Integration of CityGML and Oracle spatial for implementing 3D network analysis solutions and routing simulation within 3D-GIS environment, Geo-Spatial Inf. Sci. 16 (4) (2013) 221–237, https://doi.org/10.1080/10095020.2013.867102.
[86] I.R. Karas, S. Demir, Dijkstra algorithm interactive training software development for network analysis applications in GIS, Energy Educ. Sci. Technol. Part A Energy Sci. Res. 28 (1) (2011) 445–452.
[87] S. Ahmed, R.F. Ibrahim, H.A. Hefny, GIS-based network analysis for the roads network of the Greater Cairo area, CEUR Workshop Proc. 2144 (2017).
[88] M. Dedeoğlu, O. Dengiz, Generating of land suitability index for wheat with hybrid system aproach using AHP and GIS, Comput. Electron. Agric. 167 (2019) 105062, https://doi.org/10.1016/j.compag.2019.105062, no. October.
[89] M.S. Tehrany, B. Pradhan, M.N. Jebur, Flood susceptibility mapping using a novel ensemble weights of evidence and support vector machine models in GIS, J. Hydrol. 512 (2014) 332–343, https://doi.org/10.1016/j.jhydrol.2014.03.008.
[90] I. Elkhrachy, Flash flood hazard mapping using satellite images and GIS tools: a case study of Najran City, Kingdom of Saudi Arabia (KSA), Egypt. J. Remote Sens. Sp. Sci. 18 (2) (2015) 261–278, https://doi.org/10.1016/j.ejrs.2015.06.007.
[91] M.M. Msabi, M. Makonyo, Flood susceptibility mapping using GIS and multi-criteria decision analysis: a case of Dodoma region, Central Tanzania, Remote Sens. Appl. Soc. Environ. 21 (2021) 100445, https://doi.org/10.1016/j.rsase.2020.100445.
[92] F. Ma, et al., Soil variability description using Fourier transform mid-infrared photoacoustic spectroscopy coupling with RGB method, Catena 152 (2017) 190–197, https://doi.org/10.1016/j.catena.2017.01.005.
[93] I.E. Olorunfemi, A.A. Komolafe, J.T. Fasinmirin, A.A. Olufayo, S.O. Akande, A GIS-based assessment of the potential soil erosion and flood hazard zones in Ekiti state, Southwestern Nigeria using integrated RUSLE and HAND models, CATENA 194 (2020) 104725, https://doi.org/10.1016/j.catena.2020.104725.
[94] N. Bozali, Assessment of the soil protection function of forest ecosystems using GIS-based multi-criteria decision analysis: a case study in Adıyaman, Turkey, Glob. Ecol. Conserv. 24 (2020), e01271, https://doi.org/10.1016/j.gecco.2020.e01271.
[95] A.A. El Baroudy, Mapping and evaluating land suitability using a GIS-based model, Catena 140 (2016) 96–104, https://doi.org/10.1016/j.catena.2015.12.010.
[96] H. Kazemi, H. Akinci, A land use suitability model for rainfed farming by Multi-criteria Decision-making Analysis (MCDA) and Geographic Information System (GIS), Ecol. Eng. 116 (2018) 1–6, https://doi.org/10.1016/j.ecoleng.2018.02.021, no. March.
[97] T. Tunçay, Ş. Kılıç, M. Dedeoğlu, O. Dengiz, O. Başkan, İ. Bayramin, Assessing soil fertility index based on remote sensing and gis techniques with field validation in a semiarid agricultural ecosystem, J. Arid Environ. 190 (March, 2021), https://doi.org/10.1016/j.jaridenv.2021.104525.

HASIL CEK6_60010383

ORIGINALITY REPORT

12%	11%	3%	5%
SIMILARITY INDEX	INTERNET SOURCES	PUBLICATIONS	STUDENT PAPERS

PRIMARY SOURCES

1	www.researchgate.net Internet Source	3%
2	www.x-mol.com Internet Source	2%
3	Submitted to University of College Cork Student Paper	1%
4	www.leg.mn.gov Internet Source	1%
5	Submitted to University of Leicester Student Paper	1%
6	Submitted to Green University Of Bangladesh Student Paper	1%
7	Submitted to Institute of Technology, Tralee Student Paper	1%
8	link.springer.com Internet Source	<1%
9	www.tandfonline.com Internet Source	<1%

10	documents.mx Internet Source	<1 %
11	www.ijert.org Internet Source	<1 %
12	jurnal.fp.uns.ac.id Internet Source	<1 %
13	aut.researchgateway.ac.nz Internet Source	<1 %
14	nmhealth.org Internet Source	<1 %
15	www.ph.ucla.edu Internet Source	<1 %
16	ecologicalprocesses.springeropen.com Internet Source	<1 %
17	en.wikipedia.org Internet Source	<1 %
18	pure.ulster.ac.uk Internet Source	<1 %
19	www.frontiersin.org Internet Source	<1 %
20	E. Ustaoglu, S. Sisman, A.C. Aydınoglu. "Determining agricultural suitable land in peri-urban geography using GIS and Multi Criteria	<1 %

Decision Analysis (MCDA) techniques",
Ecological Modelling, 2021
Publication

Exclude quotes	On	Exclude matches	Off
Exclude bibliography	On		